Published in final edited form as:
Chem Res Toxicol. 2009 May ; 22(5): 918–925. doi:10.1021/tx900006b.

Formation of Mono- and Bis-Michael Adducts by the Reaction of Nucleophilic Amino Acids with Hydroxymethylvinyl Ketone, a Reactive Metabolite of 1,3-Butadiene

Nella Barshteyn and **Adnan A. Elfarra***
Department of Comparative Biosciences and Division of Pharmaceutical Sciences, University of Wisconsin, Madison, Wisconsin 53706

Abstract

Previously, our laboratory has shown that hydroxymethylvinyl ketone (HMVK), a Michael acceptor oxidation product of the 1,3-butadiene metabolite, 3-butene-1,2-diol, readily reacts with hemoglobin at physiological conditions and that mass spectrometry of trypsin digested peptides suggested adduct formation with various nucleophilic amino acids. In the present study, we characterized reactions of HMVK (3 mM) with three model nucleophilic amino acids (6 and/or 15 mM): N-acetyl-L-cysteine (NAC), L-valinamide, and N-acetyl-L-lysine (NAL). NAC was the most reactive toward HMVK followed by L-valinamide and NAL. HMVK incubations with each amino acid at pH 7.4, 37°C resulted in formation of a mono-Michael adduct. In addition, HMVK incubated with NAL gave rise to two additional bis-Michael adducts characterized by LC/MS, LC/MS/MS, ^{1}H NMR, and ^{1}H-detected heteronuclear single quantum correlation (HSQC). The relative ratios of areas of NAL monoadduct (adduct 1) and diadducts (adducts 2 and 3) at 6 h were 49, 21, and 30% of total product area, respectively. Formation of adduct 2 was dependent upon the presence of both adduct 1 and HMVK whereas formation of adduct 3 was dependent upon presence of adduct 2 only. Monoadducts were formed by a Michael addition reaction of one HMVK moiety with nucleophilic amino acid whereas NAL diadducts were products of two Michael addition reactions of 2 HMVK moieties followed by enolization and formation of an octameric cyclic product. NAL diadduct (adduct 3) was formed by loss of a water molecule from adduct 2 followed by autooxidation of one of the hydroxy groups yielding a diketone conjugated system. Collectively, our results provide strong evidence that HMVK can react with various nucleophilic residues and form different types of adducts suggesting that a variety of proteins may be subjected to these modifications which could result in loss of protein function.

Introduction

1,3-Butadiene (BD) is a petrochemical used in production of synthetic rubber and plastics. BD, which is also present in motor vehicle exhaust emissions (4.26 mg/mile) and cigarette smoke (30 to 40 μg of BD per cigarette) (1,2), has been classified by the National Toxicology Program as “known to be a human carcinogen” (3). The International Agency for Research on Cancer has upgraded BD classification to become now listed among agents that “are carcinogenic to humans” (4). Long-term inhalation exposure to BD (6.25 to 1000 ppm) has caused tumor

*To whom correspondence should be addressed: School of Veterinary Medicine 2015 Linden Drive Madison, WI 53706−1102 Telephone: (608) 262−6518 Fax: (608) 263−3926 E-mail: elfarra@svm.vetmed.wisc.edu.

Supporting Information Available
Figure S1 that contains chromatograms showing reactivity of NAL-HMVK adducts 1 and 2 and Figure S2 containing LC/MS of HMVK-valinamide adduct 3 are available in the supplemental section.
This material is available free of charge via the Internet at http://pubs.acs.org.

formation at multiple organ sites in mice and rats (5,6). Lymphocytic and myelogenous leukemias and non-Hodgkin's lymphomas have been associated with human occupational exposure (7,8). In addition, exposure to BD is associated with anemia accompanied by bone marrow toxicity and testicular and ovarian atrophy (5).

BD is readily oxidized by cytochrome P450s and myeloperoxidase to butadiene monoxide (BMO) (9,10) which can undergo hydrolysis by epoxide hydrolases to form 3-butene-1,2-diol (BDD, Figure 1). Although BDD is considered a major BD metabolite in humans and rats (11,12), only a small amount (<5%) of it was detected in the urine of rodents given BDD (13) or BMO (11). We have previously shown that BDD can be further oxidized by cytochrome P450s and alcohol dehydrogenases to yield the Michael acceptor, hydroxymethylvinyl ketone (HMVK) (13,14,15). When rats and mice were exposed to 1,3-[2,3-^{14}C]-butadiene, only 1−2% of the total globin radioactivity was characterized as trihydroxybutyl adducts, which were attributed to 1,2-dihydroxy-3,4-epoxybutane (EBD), another reactive metabolite of BD that could arise from the oxidation of BDD (Figure 1), the hydrolysis of diepoxybutane, or both (16). Because HMVK-derived mercapturates accounted for only 4−8% of the administered BDD dose (17), these results suggested that a large percentage of the BDD dose could be unaccounted for due to formation of HMVK protein adducts.

HMVK readily reacts with nucleophiles such as GSH (15) and biological macromolecules, such as Hb (18) at physiological conditions in vitro. When red blood cells were incubated with HMVK and trypsin digested globin peptides were investigated for HMVK modifications using ESI/MS, the results suggested that multiple nucleophilic amino acids including cysteine may be reacting with HMVK (18).

In the present study, we characterized the in vitro reaction of HMVK with the model nucleophilic amino acids, N-acetyl-L-lysine (NAL), L-valinamide (a model for N-terminal valine residues of Hb), and N-acetyl-L-cysteine (NAC). Interestingly, while NAC was more reactive towards HMVK than NAL, or L-valinamide and yielded a mono-Michael adduct, bis-Michael adducts and cyclic products were formed by the reaction of HMVK with NAL. These findings which demonstrate reactivity of HMVK towards different nucleophilic amino acids and the formation of different types of products, could provide insight into protein modification by HMVK after BD exposure.

Experimental Procedures

Caution

HMVK is hazardous and should be handled with care.

Materials

Butyne-1,4-diol, boron trifluoride diethyl etherate, acetone, NAC, NAL, L-valinamide, trifluoroacetic acid and deuterium oxide were purchased from Sigma-Aldrich Research (St. Louis, MO). Mercury (II) oxide and trichloroacetic acid were purchased from Fisher Scientific (Pittsburgh, PA). HMVK was synthesized as previously described (15) based on a modified Meyer-Schuster rearrangement method (19). Identity and purity was confirmed by GC/MS (Hewlett-Packard; Palo Alto, CA) (9) and H^1 NMR on Varian (Palo Alto, CA) ^{Unity}INOVA (400 MHz). HMVK purity of at least 96% was achieved consistently.

Incubations of HMVK with Model Nucleophilic Amino Acids

Reactions were performed in 10 mM PBS (8.4 mM Na_2HPO_4, 1.6 mM KH_2PO_4, 154 mM NaCl) with pH adjusted to either 4.5, 7.4, or 9.0. Reactions (8 ml-final volume) consisting of HMVK (3 mM) and NAC (6 mM) were incubated at physiological conditions (pH 7.4, 37°C)

in a shaking water bath. At each time point an aliquot was removed and set on ice before HPLC analysis. Reactions of NAL or valinamide (3 mM) with excess HMVK (6 or 15 mM) were also carried out as described above. Furthermore, the 3:15 millimolar concentration reactions were also performed at pH 7.4 (60°C), pH 4.5 (37°C), and pH 9.0 (37°C) to provide further characterization of the reaction pathway. Non-physiological conditions were used to provide insight into the structural characterization of adducts. In addition, reactions with valinamide (pH 7.4, 37°C) were carried out at the 5:1 (HMVK:amino acid) millimolar concentrations. Formation of products was monitored by HPLC (see below) over 4 or 6 h and compared against control incubations of HMVK or amino acids alone. Half-lives of HMVK under the different incubation conditions were estimated using equations for pseudo-first order elimination kinetics: $C_t = C_0 \times e^{-kt}$ and $t_{1/2} = \ln 2/k$.

HPLC Analysis of HMVK Adducts

The separation of reaction mixture components was accomplished using a Gilson HPLC system equipped with a C18 reversed-phase Beckman Ultrasphere analytical column (5μm, 4.6 mm × 25 cm) at a flow rate of 1 mL/min or a semi-preparative column (5μm, 10 mm × 25 cm) at a flow rate of 3 mL/min. UV detection was set at 220 nm. Mobile phase A was 1% acetonitrile (ACN) in double deionized water (ddH_2O), pH adjusted to 2.5 with trifluoroacetic acid (TFA); mobile phase B was 25% ACN in ddH_2O, pH adjusted to 2.5 with TFA. Initially, 0% B was maintained for 6 min. The percent B was then increased from 0 to 60 from 6 min to 10 min and held for 8 min before attaining initial conditions over 2 min and holding them for 10 min. The above method was used for time coarse reactions with NAC and valinamide on analytical and semi-preparative columns, respectively. Time course experiments for reactions with NAL were performed on semi-preparative column using the following modified method to monitor formation of adduct 2: initial 6% B, at 4.5 min increased to 60% B over 4.5 min, at 9.5 min increased to 80% B over 1 min and held for 5 min, at 15.5 min decreased to 6% B over 1.5 min and held for 9 min. The reaction products were fractionated at specific elution times using a semi-preparative column and lyophilized to dryness.

HMVK Adduct Characterization

^1H NMR analyses were performed on Varian (Palo Alto, CA) ^{Unity}INOVA or Bruker (Billerica, MA) DMX (400 MHz) at room temperature. HMVK-NAC (100% pure) adduct and HMVK-valinamide (93% pure) adduct 1 were dissolved in 0.5 ml D_2O in the following concentrations: 5.6 mg/1.0 mL and 5.8 mg/1 mL. HMVK-NAL adducts 1, 2, and 3 with respective purities of 91, 90, and 92% were also dissolved in 0.5 mL of D_2O resulting in the following concentrations: 2.6 mg/1.0 mL, 6 mg/mL, and 1.8 mg/1mL, respectively. Chemical shifts are expressed on the ppm scale using sodium 3-(trimethylsilyl)tetradeuteriopropionate as reference. HSQC (^1H-detected heteronuclear single quantum correlation) experiments with ^{13}C methanol (49.0 ppm $^{13}C \times 3.30$ ppm ^1H) serving as external reference compound were carried out using Bruker DMX (600 MHz) at the National NMR facility, University of Wisconsin-Madison. Known spectra of NAC, NAL, valinamide, HMVK, and 4-(N_α-acetyl-L-cystein-S-yl)-1-hydroxy-2-butanone (17) were used as references for structure determination.

Dried products (three HMVK-valinamide and three HMVK-NAL adducts) were redissolved in 50% ACN in ddH_2O before being subjected to ESI/MS analyses on 1100 HPLC-MSD SL Ion Trap mass spectrometer (Agilent, Santa Clara, CA) (20). The LC conditions were as described above. High-resolution mass spectrometry (HRMS) masses for HMVK-NAL adducts 2 and 3 were obtained on Varian IonSpec ProMALDI FTICR mass spectrometer.

Incubations of HMVK-NAL adducts with HMVK

Reactions of HMVK-NAL adducts 1 (2 mM) and adduct 2 (2 mM) with HMVK (2 mM) were each carried out separately in 10 mM PBS pH 7.4 at 37°C. The formation of products was

monitored over 22 h using HPLC as described above. Incubations of each adduct in the absence of HMVK were used as control.

Results

HMVK Reactivity in the Presence of Model Nucleophilic Amino Acids

When HMVK was reacted with each nucleophilic amino acid, we were able to monitor consumption of reactants and formation of products using HPLC-UV. HMVK and NAC peaks eluted at 5.7 min (Figure 2A) and 9.8 min (Figure 2B), respectively, when the analytical C18 reversed-phase column was used. To optimize resolution of peaks in reactions with NAL and L-valinamide, we used a semi-preparative column. The HMVK and NAL retention times under these conditions were at 7.1 min and 4.5 min, respectively (Figure 2C). For reactions with L-valinamide, HMVK and L-valinamide eluted at 9.4 min and 6.7 min, respectively (Figure 2D).

We monitored the stability of HMVK over 6 h and estimated its half-life when incubated alone and in the presence of each amino acid at different conditions as shown in Figures 2, 3, and Table 1. Under physiological conditions (pH 7.4, 37°C), the highest reactivity of HMVK (3 mM) was noted with NAC (6 mM) when all of HMVK was consumed at 0.5 h (Figure 3). Consumption of HMVK (3 mM) was also rapid in the presence of valinamide [HMVK $t_{1/2}$ = 16 min or 14 min at the low (6 mM) or high (15 mM) valinamide concentration, respectively] (Figure 3 and Table 1). Increasing the temperature of the incubation to 60°C favored HMVK consumption (HMVK $t_{1/2}$ = 10 min) as expected (Table 1). Under basic conditions (pH 9), 3 mM HMVK incubated with 15 mM valinamide resulted in a slightly shorter HMVK half-life (13.5 min, Table 1) than at pH 7.4 suggesting basic conditions are more favorable. Approximately 66% of HMVK (3 mM) remained unreacted 1 h after the incubation with NAL (6 mM) at physiological conditions, thus, half-life of HMVK was estimated as the longest (HMVK $t_{1/2}$ = 105 min) in comparison to reactions with NAC or valinamide (Figure 3, Table 1). The NAL reaction rate increased (HMVK $t_{1/2}$ = 55 min) at the high NAL concentration (15 mM) and at 60°C (HMVK $t_{1/2}$ = 8.6 min) (Table 1) with 44% and 2% of HMVK, respectively, remaining unreacted at 1 h. At pH 9.0, the rate of HMVK consumption was faster than at pH 7.4 (Table 1) with 33% of HMVK remaining unreacted at 1 h.

Formation and Characterization of HMVK-NAC Adduct

Upon incubating HMVK (3 mM) with NAC (6 mM) at physiological conditions (pH 7.4, 37° C), instantaneous formation of one major product at 12.5 min was detected (Figures 2B and 4A) demonstrating high reactivity of HMVK with NAC. ^{1}H NMR data summarized in Table 2 confirmed an adduction of 1 HMVK moiety to NAC as shown in Figure 5A. The spectrum was consistent with a previously characterized mercapturic acid urinary metabolite of BDD, 4-(N_α-acetyl-L-cystein-S-yl)-1-hydroxy-2-butanone (17).

Formation of HMVK-NAL Adducts

Upon incubating HMVK (3 mM) with NAL (15 mM) at physiological conditions (pH 7.4, 37° C), a time-dependent formation of three adducts was detected (Figures 2C and 4B). The products were designated as adducts 1, 2, and 3 based on the order of their HPLC retention times (Figure 2C). As discussed below, peaks eluting at 6.5 and 6.7 min represent stereoisomers of adduct 2. Adduct 1 was formed after 0.5 h of incubation whereas adducts 2 and 3 were detectable at 1h (Figure 4B). The area of adduct 1 doubled at 1 h. The rates of formation of adducts 1 and 2 slowed down significantly after the first 2 hours of incubation whereas the rate of formation of adduct 3 was linear in between 2 and 6 h (Figure 4B). Because HMVK consumption did not change in between these time points (Figure 3), the data suggested that formation of adduct 3 may depend on formation of adducts 1 or 2. The lower yield of adduct 2 as compared to adduct 1 and its higher yield at earlier time points as compared to adduct 3

(Figure 4B) provided support for this hypothesis. The typical relative ratios of areas of adducts 1−3 at 6 h were as follows: 49, 21, and 30% of total product area, respectively (Figure 4B). When the HMVK-NAL reaction was carried out at basic conditions (pH 9.0) or at higher temperature (pH 7.4, 60°C), the relative ratios of areas for adducts 1−3 at 6 h (40, 24, and 36% and 32, 18, and 50% of total product area, respectively), suggested a higher preference for formation of adduct 3 as compared to ratios observed at pH 7.4 at 37°C.

Stability and Reactivity of HMVK-NAL Adducts

To provide evidence for whether adducts 1 and/or 2 give rise to adduct 3, we incubated adducts 1 and 2 (2 mM) separately with and without HMVK (2 mM) at physiological conditions (pH 7.4, 37°C). The results demonstrated that adduct 1 gave rise to adducts 2 and 3 only in the presence of HMVK (Supporting Information, Figure S1A and B) providing evidence that adduct 1 is the precursor to both adducts 2 and 3. Adduct 2 gave rise to adduct 3 at 7 h in the absence of HMVK (Supporting Information, Figure S1C) suggesting that it is the immediate precursor to adduct 3.

Structural Characterization of HMVK-NAL Adducts

The HMVK-NAL reaction mixtures were fractionated by HPLC and each product peak was lyophilized before being analyzed by ESI/MS and ^{1}H NMR (Table 3). ^{1}H NMR spectra for NAL and HMVK served as references for structure determination of these adducts. Adduct 1 exhibited characteristic molecular ion peak at m/z 275.0 in positive mode (Figure 6A). MS/MS of the molecular ion revealed molecular fragments at m/z 201.0 and 155.0 that correspond to the loss of CH_3COCH_2OH and cleavage of formic acid from NAL, respectively, (Figure 6B). Adduct 1 was ascertained by ^{1}H NMR (Table 3) and MS to be consistent with 1 HMVK moiety adducted to the free amino end of NAL as shown in Figure 7.

HRMS for adduct 2 (peak at 6.5 min, Figure 2C) exhibited a characteristic molecular ion peak of 361.19512 Da (calculated 361.19693 Da, Figure 6C) corresponding to $C_{16}H_{29}N_2O_7^{+1}$ consistent with formation of the cyclic product shown in Figure 7. MS/MS of the molecular ion peak displayed fragment ions at m/z 343.1, 325.0, 307.1 corresponding to the loss of 1, 2, or 3 water molecules (Figure 6D). The latter eluting peak of adduct 2 (at 6.7 min, Figure 2C) was determined to be a stereoisomer of the earlier eluting peak based upon similar MS and MS/MS spectra (data not shown) and the lack of consistent resolution of these two peaks between experiments. Integration of ^{1}H NMR (Table 3) data of adduct 2 (at 6.5 min) revealed a higher proton number consistent with addition of 2 HMVK moieties. Adduct 3 displayed a molecular ion peak of 341.17120 Da (calculated 341.17071 Da, Figure 6E) by HRMS corresponding to $C_{16}H_{25}N_2O_6^{+1}$. MS/MS of the molecular ion peak exhibited fragment ions at m/z 323.1, 295.1, and 281.0 that correspond to loss of a water molecule, cleavage of formic acid from NAL, and loss of $CH_3CONH_3^+$ from NAL, respectively (Figure 6F). Representative ^{1}H NMR and HSQC spectra for adduct 3 are shown in Figures 8A and B, respectively. Based on HSQC experiment, tentative assignments of ring CH_2 protons (δ3.65, δ2.96, δ3.15) were correlated to C-9, C-10 and C-15, respectively, taking into account the electron-withdrawing environment surrounding each CH_2 group (Table 3). These groups have similar shifts for adducts 2 (peak at 6.5 min, Figure 2C) and 3 as shown by ^{1}H NMR suggesting no structural differences between these adducts in that part of the ring. However, a singlet at 2.6 ppm consisting of 1 H in adduct 2 and lack of such singlet in adduct 3 suggests the presence of a CH group without any protons nearby as shown for C-12 in Figure 7. Both ^{1}H NMR and HSQC revealed the expected shifts of the vinylic proton and the vinylic carbon (C-14), respectively, to be more downfield in adduct 3 than the respective C-14 in adduct 2 which contains no double bond in the ring structure. Furthermore, C-16 is similarly affected by the electron withdrawing nature of the nearby double bond located α,β to the carbonyl in adduct 3 with its proton shift more downfield than in adduct 2. Thus, adducts 2 and 3 are confirmed

to be diadducts consisting of 1 NAL and 2 HMVK moieties with different ring functional groups (Figure 7).

Formation of HMVK-Valinamide Adducts

Upon incubating HMVK (3 mM) with valinamide (15 mM) at physiological conditions (pH 7.4, 37°C), a time-dependent formation of one major (adduct 1, with 90 % of total product area at 4 h) and two minor products (adduct 2 and adduct 3) was observed (Figure 2D and 4C). Adduct 1 was already detectable at time 0 remaining at plateau for the duration of the incubation. Formation of adducts 2 and 3, however, was observed 30 min later and their areas continued to increase between 1 and 4 h. The relative areas of adducts 2 and 3 increased whereas the relative area of adduct 1 decreased when the reaction was carried out at a higher HMVK:valinamide (5:1) millimolar ratio or when the HMVK:valinamide (3:15 mM) was carried out at 37°C, pH 9.0 (data not shown).

Characterization of HMVK-Valinamide Adducts

After the reaction mixture was fractionated by HPLC and each product peak lyophilized, adduct 1 was subjected to ESI/MS and ^{1}H NMR (Table 2) and adducts 2 and 3 were analyzed by ESI/MS alone. ^{1}H NMR spectra for valinamide and HMVK served as references to determine the structure of adduct 1. Adduct 1 was characterized as 1 HMVK moiety adducted to the free amino group of valinamide as shown in Figure 5B. The mass spectrum exhibited characteristic fragment ions at m/z 203.0 and 128.9 in positive mode corresponding to M+1 and loss of CH_3COCH_2OH respectively (Figure 9A). MS/MS spectrum of m/z 203.0 ion showed fragments m/z 158.1 and m/z 117.3 in addition to m/z 128.9 that correspond to the loss of an amide moiety and loss of HMVK, respectively (Figure 9B). We were unable to maintain stability of adduct 2 to produce useful ESI/MS data. However, mass spectrum of adduct 3 exhibited a molecular ion peak at m/z 269.2 (Supporting Information, Figure S2) consistent with the expected mass for the cyclic diadduct that may be formed by a mechanism (cyclization of the valinamide-diadduct followed by loss of H_2O and autooxidation) similar to that described in Figure 7 for adduct 3 in reactions of HMVK with NAL. Ion at m/z 287.0 may represent the other cyclic diadduct (before water molecule loss) similar to adduct 2 described in reactions with NAL.

Discussion

In characterizing reactivity of HMVK with model nucleophilic amino acids, we demonstrated that HMVK reacts via Michael addition preferentially with sulfhydryl groups followed by amino groups. Preference for the reaction of these amino acids toward HMVK occurred in the following order: NAC > valinamide > NAL (Figure 3A). Other Michael acceptors, such as 4-hydroxynonenal and 4-oxononenal, exhibited a similar preference for cysteine over lysine (21).

All three amino acids gave rise to HMVK monoadducts suggesting that a wide variety of macromolecules are potential targets for HMVK in vivo. Proposed mechanism for formation of monoadducts (HMVK-NAC adduct, HMVK-NAL adduct 1, and HMVK-valinamide adduct 1) involves nucleophilic addition of amino acid to the terminal vinylic carbon of HMVK as shown in Figures 5 and 7. The dissolution of the double bond is evidenced by ^{1}H NMR spectra (Tables 2 and 3) that lack the presence of the three protons associated with double bond of HMVK expected at a much higher downfield shift (6−7 ppm). The proton shifts/integrations corresponding to the known spectra of model amino acids used in this study and HMVK protons (not involved in the double bond) along with MS and MS/MS data (for HMVK-NAL and HMVK-valinamide monoadducts) led us to define the structures of the monoadducts.

The proposed mechanism for HMVK-NAL adduct 2 formation is initiated by formation of HMVK monoadduct with the ε-amino group of NAL as described above and shown for adduct 1 (Figure 7). This secondary amine intermediate (or adduct 1) further reacts with another HMVK molecule to result in the bis-Michael adduct. Reactivity of HMVK was accelerated at basic pH promoting a more favorable nucleophilic attack likely due to deprotonation of the amino groups of NAL (and valinamide) permitting addition of a second molecule of HMVK. The resulting intermediate was not detected probably due to its instability and immediate fusion of HMVK molecules via enolization to form the octameric ring structure. Although molecular ion mass for NAL-HMVK adduct 2 did not allow differentiation between addition of 2 moieties of HMVK that remain intact or the fused derivative of these molecules to form an 8-membered ring structure, ^{1}H NMR and MS/MS led to characterization of adduct 2 as an octameric cyclic diadduct. MS/MS spectra suggested a loss of 3 water molecules corresponding to the 3 hydroxyl groups present in the structure and ^{1}H NMR displayed additional peaks not observed with the monoadduct and demonstrated similarity in the shifts of protons of C-9, C-10, and C-15 to the ring structure of adduct 3. Previously, lysine was shown to undergo a similar mechanism involving addition of two molecules of acrolein, another α,β-unsaturated compound, to produce Nε-(3-formyl-3,4-dehydropiperidino)lysine (FDP) derivative (22). The secondary amine intermediate carrying two intact acrolein molecules was also postulated unstable (22).

We characterized HMVK-NAL adduct 3 as a different type of HMVK-derived diadduct consisting of an octameric cyclic diketone stucture formed when adduct 2 had undergone loss of water from C-13 leading to the formation of a ring double bond. Autooxidation of one of the hydroxy groups follows which is more likely to occur at C-12 position than at the allylic alcohol (C-16) yielding a diketone conjugated system. A similar mechanism was elucidated with ketol that had undergone enolization to a hydroquinone and spontaneously autooxidized to o-quinone (23). Although we did not confirm the identity of HMVK-valinamide adduct 3 by NMR as we did in our characterization of HMVK-NAL adduct 3, its favored formation with higher HMVK concentration (data not shown) along with the MS data suggest that adduct 3 may also be a cyclic diadduct. The reaction pathway for diadduct formation delineated in this study was also supported by not detecting HMVK dimers under the conditions we used. Consequently, because no dimer adducts were detected with NAC, these results suggest that NAL and valinamide cyclic diadducts were not formed by reaction of an HMVK dimer with NAL or valinamide.

Cysteines and lysines are nucleophilic residues ubiquitous in many proteins that upon reaction with electrophilic compounds could potentiate disturbance of redox state of cells (GSH depletion) and/or alter protein function causing cellular toxicity. Cysteines are key catalytic components that facilitate enzyme function and have metal binding ability. Thioredoxins and glutathione reductase are examples of cysteine-containing proteins that rely on the reduced state of cysteine for their activity (24) which could be compromised if reactive electrophiles, such as HMVK are present. In this regard, peroxynitrite was shown to irreversibly inactivate N-acetyltransferase 1 in human breast cancer cells due to oxidative modification of the catalytic cysteine residue (25). Proteins containing lysines in the active site are also targets for modifications by reactive electrophiles. The loss of activity of glucose-6-phosphate dehydrogenase was observed upon incubation with 4-hydroxy-2-nonenal (HNE), another Michael acceptor, and formation of HNE-lysine adduct was detected (26). As is the case with FDP-lysine which was shown to undergo further reactions with GSH (27), the α,β-unsaturated carbonyl moiety is retained in adduct 3 (Figure 7) making C14 vulnerable for further potential nucleophilic attacks. This reaction could further deplete GSH and potentiate further redox instability in cells. Alternatively, cross-linking with other proteins may also occur leading to cellular dysfunction. FDP-lysine-mediated cross-links were shown to promote protein aggregation in Parkinson's disease (28).

Although internal valine residues in proteins are not sites of modification by electrophiles, N-terminal valine in Hb is commonly used in biomonitoring exposure to electrophilic metabolites of various chemicals, including BD. The levels of Hb adduct formation with reactive intermediates of BD were correlated to toxicity/carcinogenicity (29). Thus, reactivity of HMVK with multiple nucleophilic residues in Hb, including cysteine, lysine, and N-terminal valine, could help explain why only a small fraction of the radioactivity bound to Hb was attributed to EBD after BD exposure (16). Although we limited our study to three nucleophilic amino acids, other nucleophilic residues, such as histidines, arginines, and methionines could serve as additional targets for reactivity with HMVK.

In conclusion, we have characterized chemical reactivity of HMVK toward nucleophilic amino acid derivatives at different ratios and incubation conditions with NAC showing the most reactive potential followed by valinamide and NAL. HMVK readily reacts with all three nucleophiles to yield monoadducts via a classical Michael addition reaction suggesting that a variety of proteins may be subjected to modifications by HMVK in vivo. In addition, reaction with NAL yielded two types of diadducts consisting of two HMVK moieties providing another way that HMVK could interact with biological nucleophiles. Further investigation of protein adducts with HMVK is warranted to gain more insight into the mechanisms involved in the toxicity and carcinogenicity of BD.

Supplementary Material

Refer to Web version on PubMed Central for supplementary material.

Acknowledgment

This research was made possible by Grant DK044295 from the National Institutes of Health. N.B. was supported by an institutional training grant from NIEHS (T32-ES-007015)

Abbreviations

ACN, acetonitrile
BD, 1,3-Butadiene
BDD, 3-butene-1,2-diol
BMO, butadiene monoxide
ddH_2O, double deionized water
EBD, 1,2-dihydroxy-3,4-epoxybutane
FDP lysine, Nε-(3-formyl-3,4-dehydropiperidino)lysine
HMVK, hydroxymethylvinyl ketone
HSQC, ^{1}H-detected heteronuclear single quantum correlation
HRMS, High Resolution Mass Spectrometry
HNE, 4-hydroxy-2-nonenal
NAC, N-acetyl-L-cysteine
NAL, N-acetyl-L-lysine
TFA, trifluoroacetic acid

References

1. Hesterberg TW, Lapin CA, Bunn WB. A comparison of emissions from vehicles fueled with diesel or compressed natural gas. Environ. Sci. Technol 2008;42:6437–6445. [PubMed: 18800512]
2. Adam T, Mitschke S, Streibel T, Baker RR, Zimmermann R. Quantitative puff-by-puff resolved characterization of selected toxic compounds in cigarette mainstream smoke. Chem. Res. Toxicol 2006;19:511–520. [PubMed: 16608162]

3. National Toxicology Program (NTP). Report on Carcinogens. Vol. 11th ed. U.S. Department of Health and Human Services, Public Health Service, National Toxicology Program; Research Triangle Park, NC: 2005.
4. Grosse Y, Baan R, Straif K, Secretan B, El Ghissassi F, Bouvard V, Altieri A, Cogliano V. Carcinogenicity of 1,3-butadiene, ethylene oxide, vinyl chloride, vinyl fluoride, and vinyl bromide. Lancet Oncol 2007;8:679–680. [PubMed: 17726789]
5. Melnick RL, Huff JE, Roycroft JH, Chou BJ, Miller RA. Inhalation toxicology and carcinogenicity of 1,3-butadiene in B6C3F1 mice following 65 weeks of exposure. Environ. Health Perspect 1990;86:27–36. [PubMed: 2401263]
6. Owen PE, Glaister JR, Gaunt IF, Pullinger DH. Inhalation toxicity studies with 1,3-butadiene. 3. Two year toxicity/carcinogenity study in rats. Am. Ind. Hyg. Assoc. J 1987;48:407–413. [PubMed: 3591659]
7. Graff JJ, Sathiakumar N, Macaluso M, Maldonado G, Matthews R, Delzell E. Chemical exposures in the synthetic rubber industry and lymphohematopoietic cancer mortality. J. Occup. Environ. Med 2005;47:916–932. [PubMed: 16155477]
8. Ward EM, Fajen JM, Ruder AM, Rinsky RA, Halperin WE, Fessler-Flesch CA. Mortality study of workers in 1,3-butadiene production units identified from a chemical workers cohort. Environ. Health Perspect 1995;103:598–603. [PubMed: 7556014]
9. Duescher RJ, Elfarra AA. Human liver microsomes are efficient catalysts of 1,3-butadiene oxidation: evidence for major roles by P450 2A6 and 2E1. Arch. Biochem. Biophys 1994;311:342–349. [PubMed: 8203896]
10. Duescher RJ, Elfarra AA. 1,3-Butadiene oxidation of human myeloperoxidase: role of chloride ion in catalysis of divergent pathways. J. Biol. Chem 1992;267:19859–19865. [PubMed: 1328183]
11. Krause RJ, Sharer JE, Elfarra AA. Epoxide hydrolase-dependent metabolism of butadiene monoxide to 3-butene-1,2-diol in mouse, rat, and human liver. Drug Metab. Dispos 1997;25:1013–1015. [PubMed: 9280411]
12. Bechtold WE, Strunk MR, Chang IY, Ward JB, Henderson RF. Species differences in urinary butadiene metabolites: comparisons of metabolite ratios between mice, rats, and humans. Toxicol. Appl. Pharmacol 1994;127:44–49. [PubMed: 8048052]
13. Kemper RA, Elfarra AA, Myers SR. Metabolism of 3-butene-1,2-diol in B6C3F1 mice: evidence for involvement of alcohol dehydrogenase and cytochrome P450. Drug Metab Dispos 1998;26:914–920. [PubMed: 9733671]
14. Kemper RA, Elfarra AA. Oxidation of 3-butene-1,2-diol by alcohol dehydrogenase. Chem. Res. Toxicol 1996;96:1127–1134. [PubMed: 8902267]
15. Krause RJ, Kemper RA, Elfarra AA. Hydroxymethylvinyl ketone: a reactive Michael acceptor formed by the oxidation of 3-butene-1,2-diol by cDNA-expressed human cytochrome P450s and mouse, rat, and human liver microsomes. Chem. Res. Toxicol 2001;14:1590–1595. [PubMed: 11743741]
16. Booth ED, Kilgour JD, Watson WP. Dose responses for the formation of hemoglobin adducts and urinary metabolites in rats and mice exposed by inhalation to low concentrations of 1,3-[2,3-^{14}C]-butadiene. Chem. Biol. Interact 2004;147:213–232. [PubMed: 15013822]
17. Sprague CL, Elfarra AA. Mercapturic acid urinary metabolites of 3-butene-1,2-diol as in vivo evidence for the formation of hydroxymethylvinyl ketone in mice and rats. Chem. Res. Toxicol 2004;17:819–826. [PubMed: 15206903]
18. Barshteyn N, Krause RJ, Elfarra AA. Mass spectral analyses of hemoglobin adducts formed after in vitro exposure of erythrocytes to hydroxymethylvinyl ketone. Chem. Biol. Interact 2007;166:176–181. [PubMed: 16735035]
19. Swaminathan S, Narayanan KV. The Rupe and Meyer-Schuster Rearrangements. Chem. Rev 1971;71:429–438.
20. Barshteyn N, Elfarra AA. Formation of three N-acetyl-L-cysteine monoadducts and one diadduct by the reaction of S-(1,2-dichlorovinyl)-L-cysteine sulfoxide with N-acetyl-L-cysteine at physiological conditions: chemical mechanisms and toxicological implications. Chem. Res. Toxicol 2007;20:1563–1569. [PubMed: 17892265]
21. Doorn JA, Petersen DR. Covalent adduction of nucleophilic amino acids by 4-hydroxynonenal and 4-oxononenal. Chem. Biol. Interact 2003;143−144:93–100.

22. Uchida K, Kanematsu M, Morimitsu Y, Osawa T, Noguchi N, Niki E. Acrolein is a product of lipid peroxidation reaction. Formation of free acrolein and its conjugate with lysine residues in oxidized low-density lipoproteins. J. Biol. Chem 1998;273:16058–16066. [PubMed: 9632657]

23. Smithgall TE, Harvey RG, Penning TM. Spectroscopic Identification of ortho-quionones as products of polycyclic aromatic trans-dihydrodiol oxidation catalyzed by dihydrodiol dehydrogenase. J. Biol. Chem 1988;263:1814–1820. [PubMed: 3276678]

24. Giles NM, Watts AB, Giles GI, Fry FH, Littlechild JA, Jacob C. Metal and redox modulation of cysteine protein function. Chem. Biol 2003;10:677–693. [PubMed: 12954327]

25. Dairou J, Atmane N, Rodrigues-Lima F, Dupret J. Peroxynitrite irreversibly inactivates the human xenobiotic-metabolizing enzyme arylamine N-acetyltransferase 1 (NAT1) in human breast cancer cells. A cellular and mechanistic study. J. Biol. Chem 2004;279:7708–7714. [PubMed: 14672957]

26. Szweda LI, Uchida K, Tsai L, Stadtman ER. Inactivation of glucose-6-phosphate dehydrogenase by 4-hydroxy-2-nonenal. J. Biol. Chem 1993;268:3342–3347. [PubMed: 8429010]

27. Furuhata A, Nakamura M, Osawa T, Uchida K. Thiolation of protein-bound carcinogenic aldehyde. An electrophilic acrolein-lysine adduct that covalently binds to thiols. J. Biol. Chem 2002;277:27919–27926. [PubMed: 12032148]

28. Shamoto-Nagai M, Maruyama W, Hashizume Y, Yoshida M, Osawa T, Riederer P, Naoi M. In parkinsonian substantia nigra, alpha-synuclein is modified by acrolein, a lipid-peroxidation product, and accumulates in the dopamine neurons with inhibition of proteasome activity. J. Neural Transm 2007;114:1559–1567. [PubMed: 17690948]

29. Swenberg JA, Christova-Gueorguieva NI, Upton PB, Ranasinghe A, Scheller N, Wu K, Yen T, Hayes R. 1,3-Butadiene: cancer, mutations, and adducts. Part V: hemoglobin adducts as biomarkers of 1,3-butadiene exposure and metabolism. Res. Rep. Health Eff Inst 2000;92:191–210. [PubMed: 10925842]

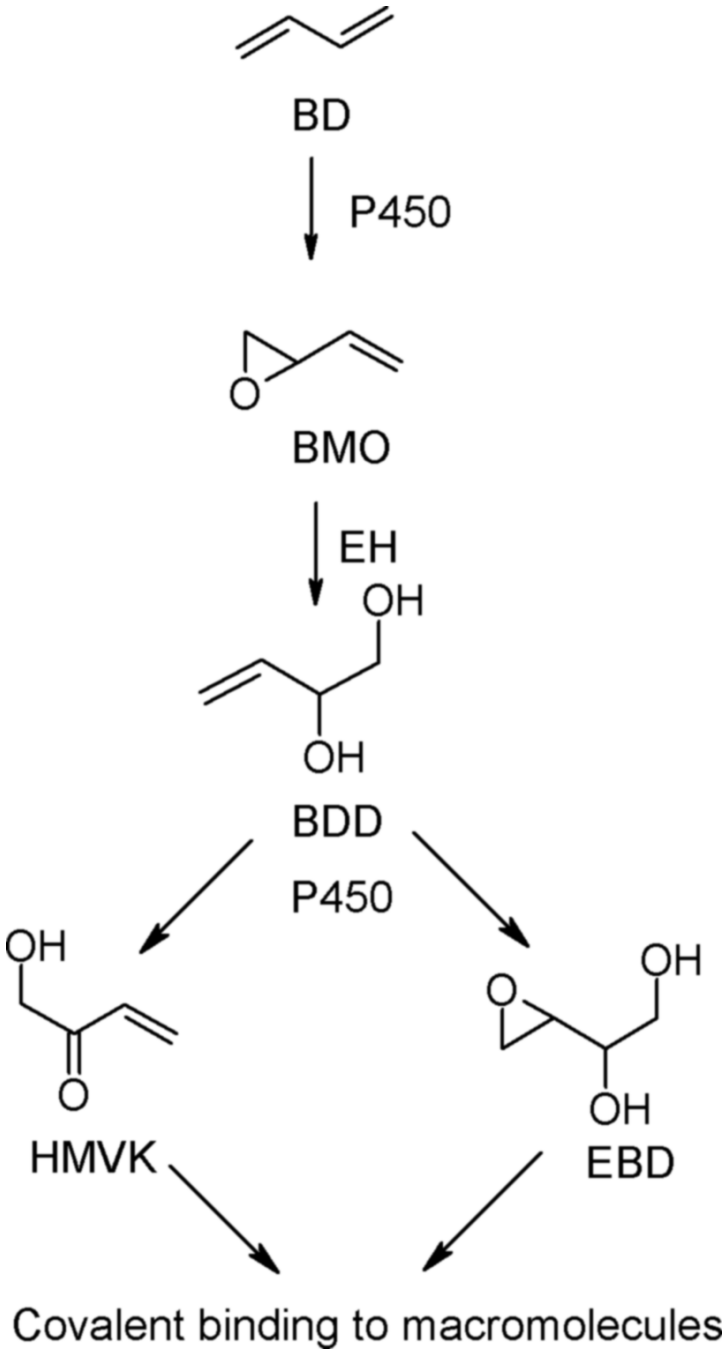

Figure 1.
Scheme of 1,3-butadiene (BD) metabolism. Butadiene monoxide (BMO), 3-Butene-1,2-Diol (BDD), Hydroxymethylvinyl ketone (HMVK), 1,2-dihydroxy-3,4-epoxybutane (EBD), Epoxide hydrolase (EH).

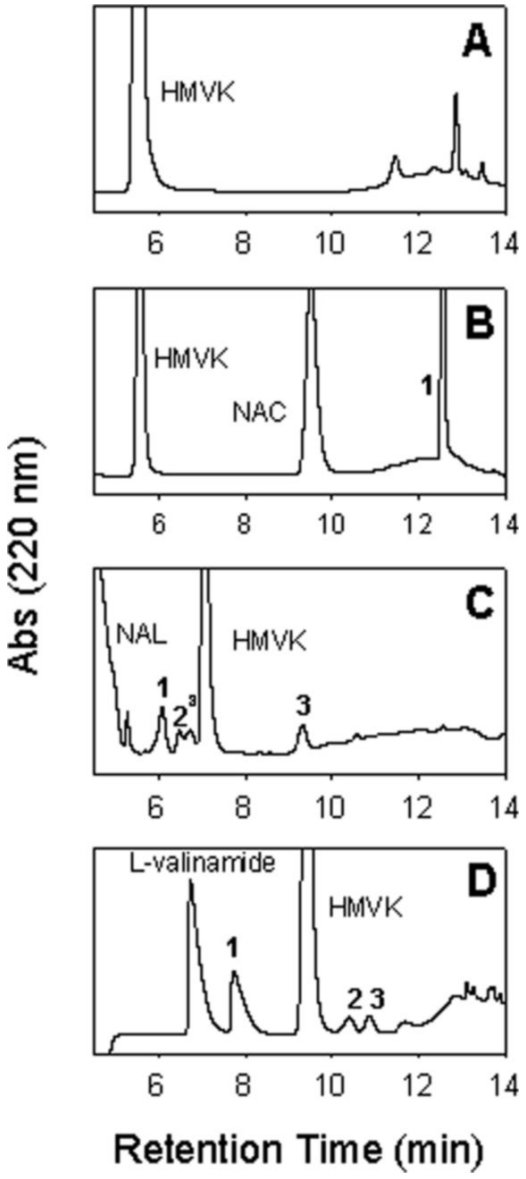

Figure 2.

Typical chromatograms of HMVK incubated with nucleophilic amino acids at pH 7.4, 37°C for 6 h. (A) 3 mM HMVK. (B) 3 mM HMVK with 6 mM NAC. Peak 1 refers to HMVK-NAC adduct (C) 3 mM HMVK with 15 mM NAL. Peaks 1, 2, and 3 refer to HMVK-NAL adducts 1, 2, and 3, respectively. [a]both peaks represent stereoisomers of adduct 2 as confirmed by ESI/MS (D) 3 mM HMVK with 15 mM L-valinamide. Peaks 1, 2, and 3 refer to HMVK-valinamide adducts 1, 2, and 3, respectively. HPLC methods using analytical column (Panels A and B) or semi-preparative column (Panels C and D) included gradient starting at 0% (Panels A, B, and D) or 6% (Panel C) of mobile phase B as described in the Experimental Procedures.

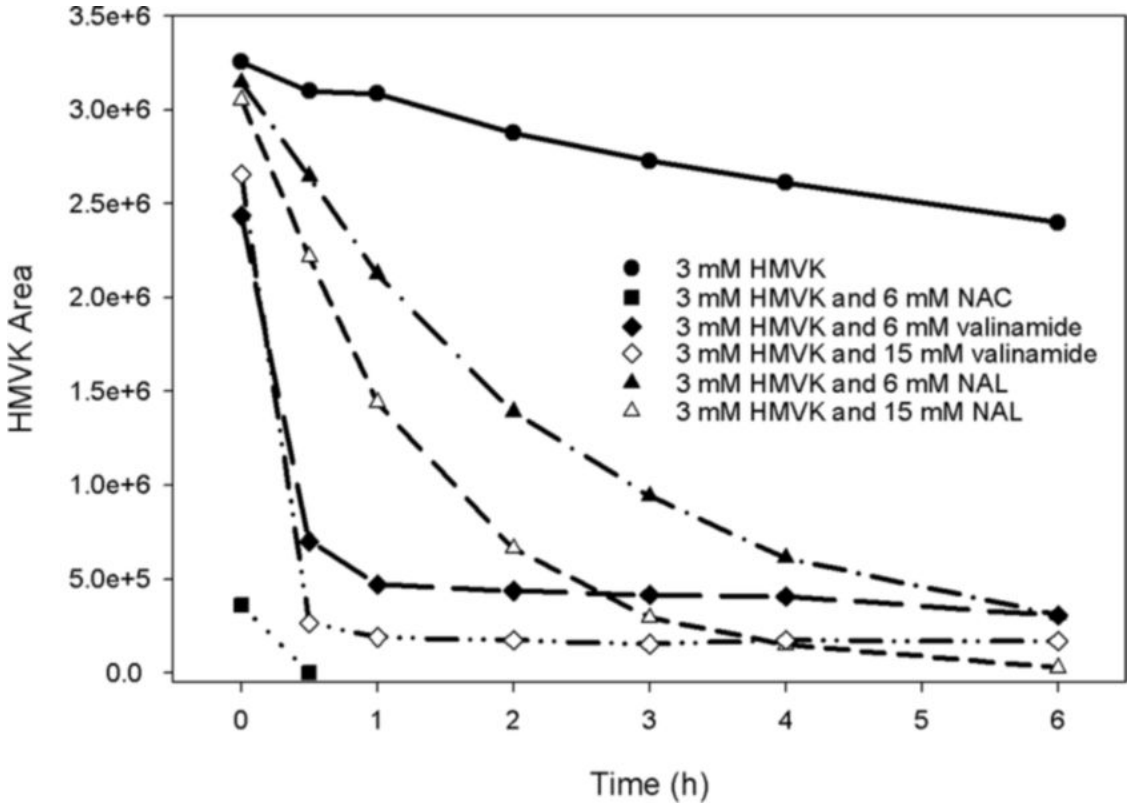

Figure 3.
(A) Stability of HMVK alone and in reactions with NAC, valinamide, and NAL at pH 7.4, 37° C at different reactant ratios.

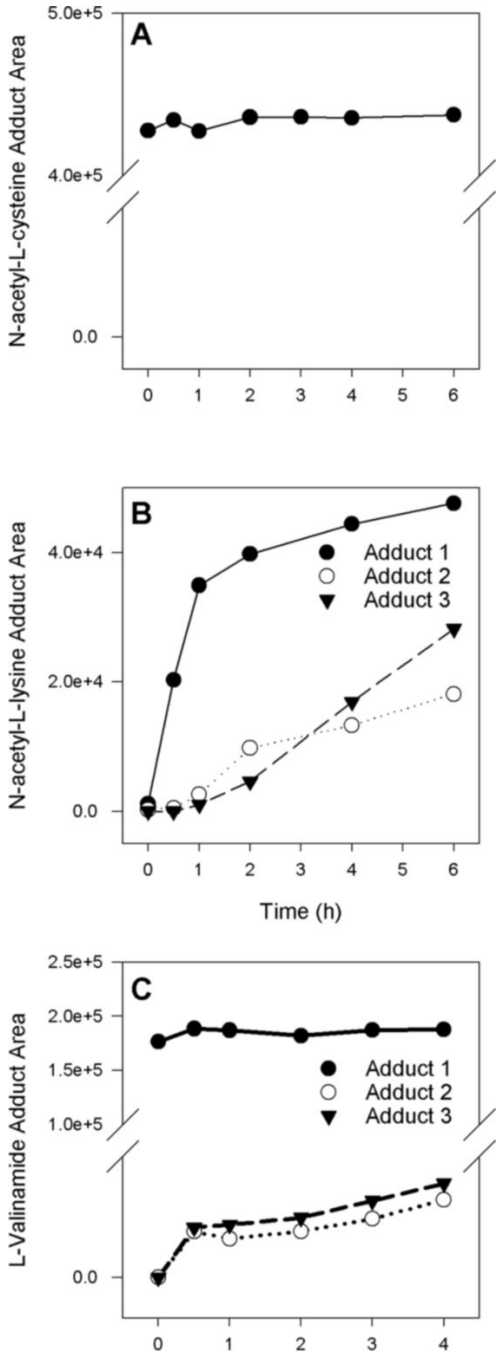

Figure 4.

(A) Formation of HMVK-NAC adduct over time at a reaction ratio of 3 mM HMVK to 6 mM NAC. (B) Formation of HMVK-NAL adducts 1−3 over time at a reaction ratio of 3 mM HMVK to 15 mM NAL. (C) Formation of HMVK-valinamide adducts 1−3 over time at a reaction ratio of 3 mM HMVK to 15 mM valinamide. N-acetyl-L-cysteine (NAC), N-acetyl-L-lysine (NAL).

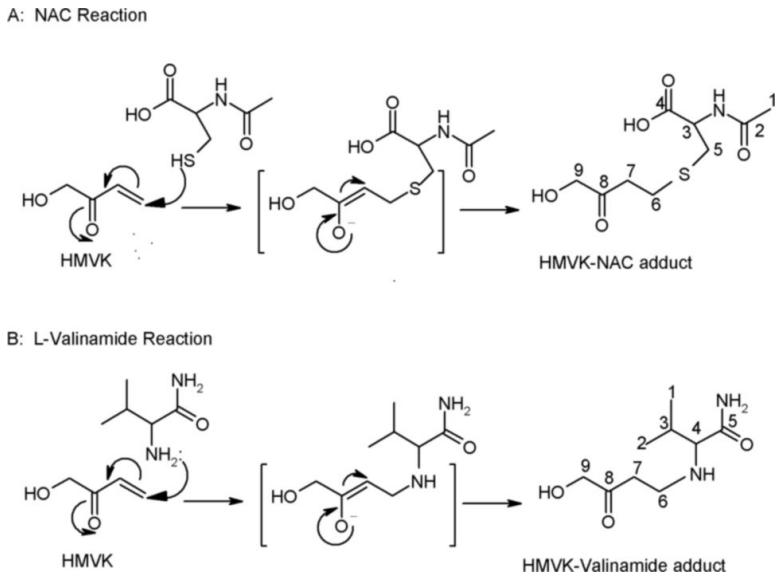

Figure 5.
Proposed mechanism for formation of HMVK monoadducts with (A) NAC and (B) L-valinamide.

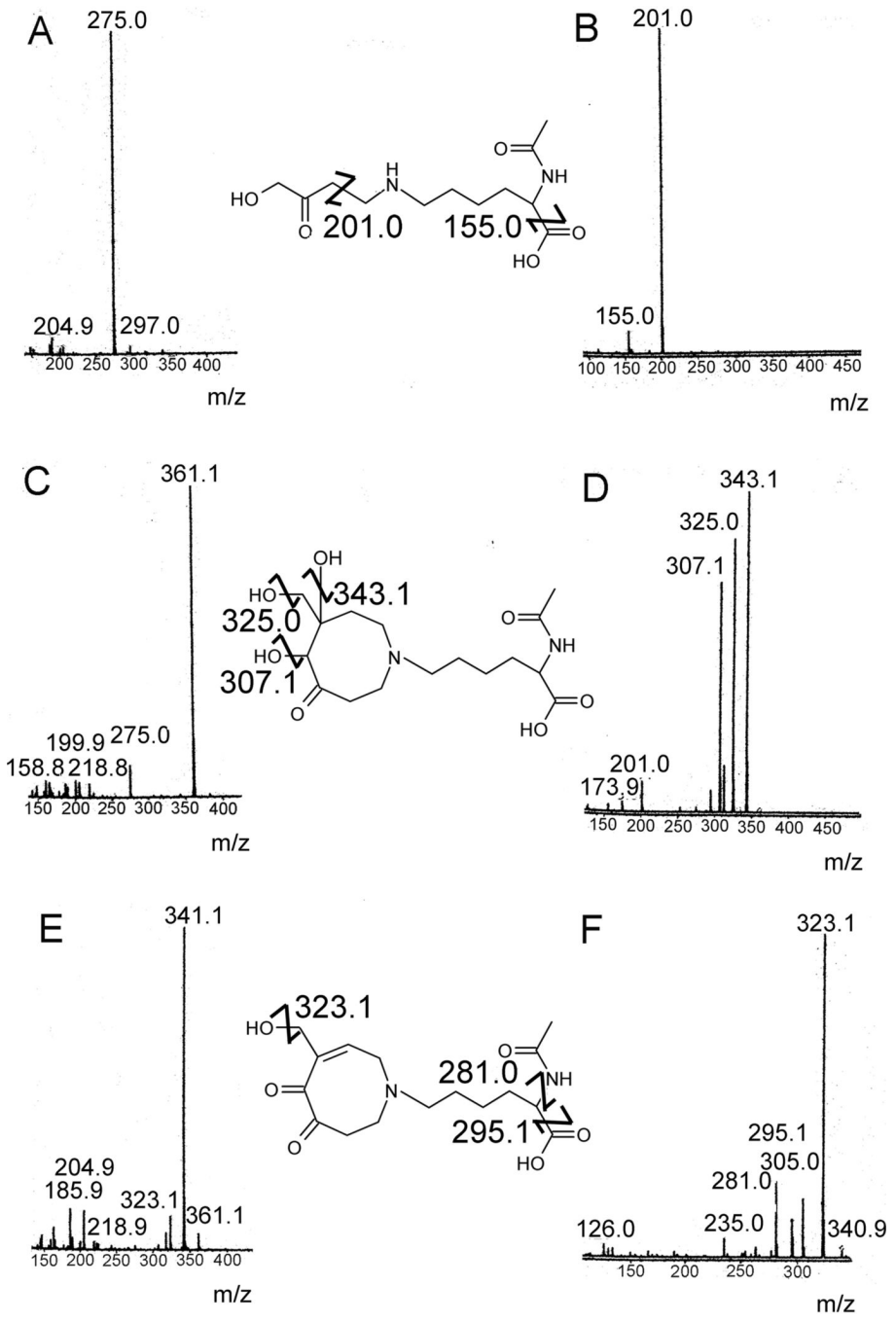

Figure 6.

(A) LC/MS (B) LC/MS/MS of HMVK-NAL monoadduct (adduct 1). (C) LC/MS (D) LC/MS/MS of HMVK-NAL diadduct (adduct 2) (E) LC/MS (F) LC/MS/MS of HMVK-NAL diadduct (adduct 3).

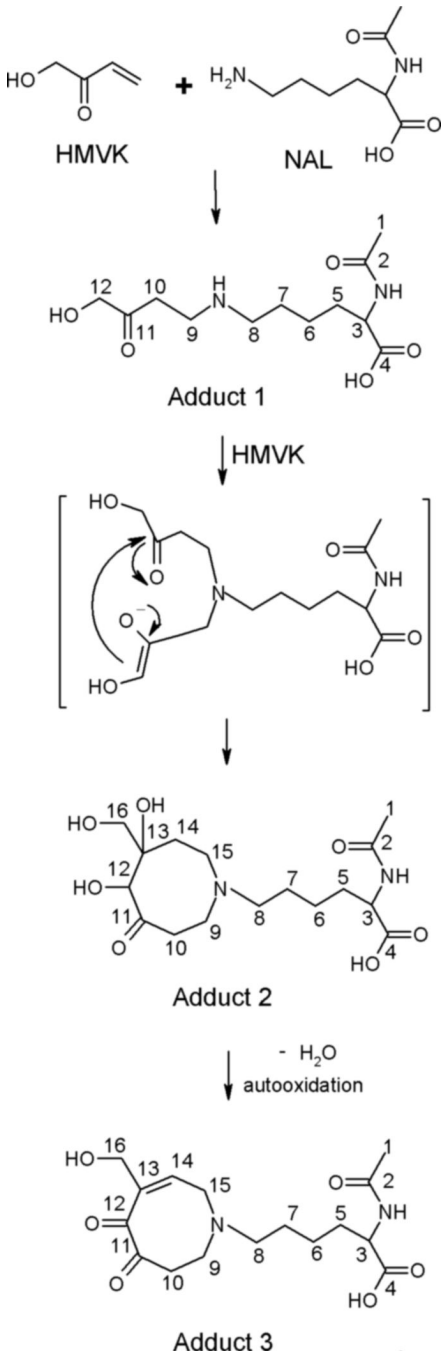

Figure 7.
Proposed mechanism for formation of HMVK adducts 1−3 with NAL. HMVKNAL monoadduct (adduct 1), HMVK-NAL diadduct (adduct 2), HMVK-NAL diadduct (adduct 3).

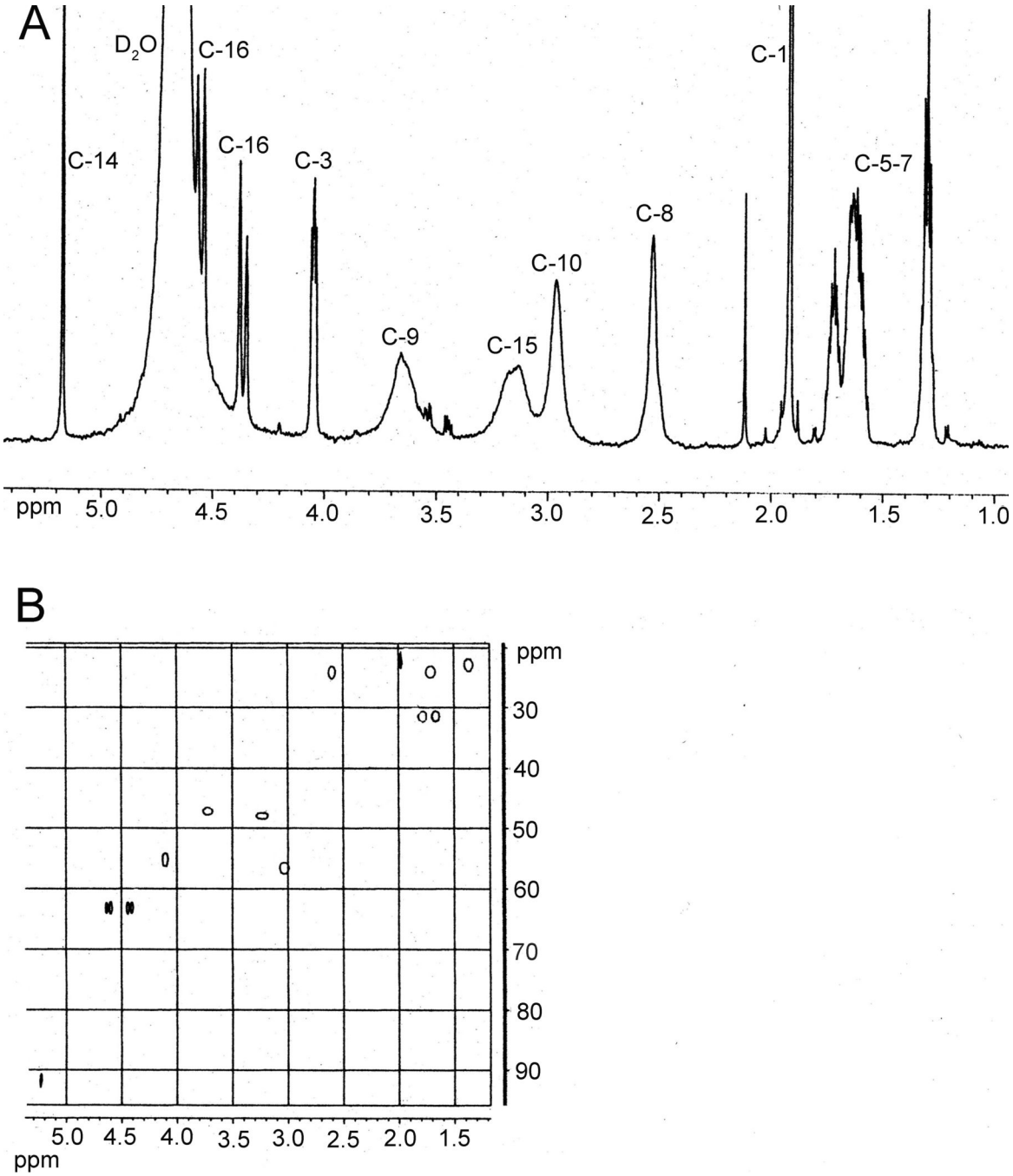

Figure 8.
(A) 400 Hz ^{1}H NMR (B) 600 Hz HSQC of HMVK-NAL diadduct (adduct 3). The chemical structure is shown in Figure 7.

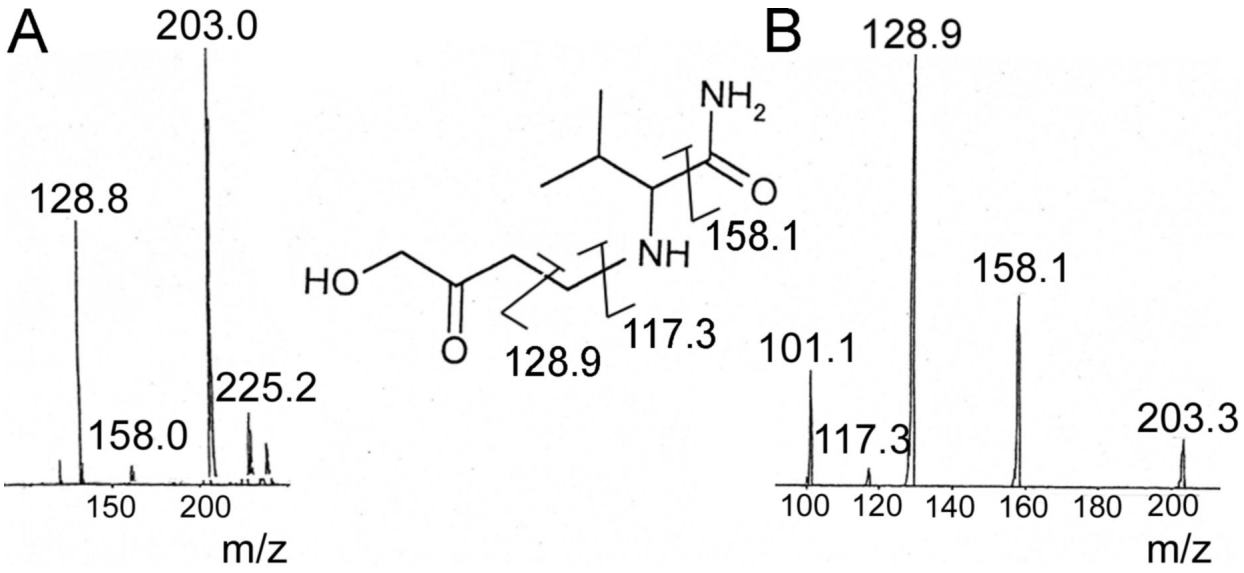

Figure 9.
(A) LC/MS (B) LC/MS/MS of HMVK-valinamide adduct 1.

Table 1

Estimated Half-lives (min) of HMVK in the Presence of NAC, NAL, or L-valinamide

HMVK[a]:AA (mM concentrations)	HMVK + NAC	HMVK + NAL			HMVK + L-valinamide		
	pH 7.4 37 °C	pH 7.4 37 °C	pH 9 37 °C	pH 7.4 60 °C	pH 7.4 37 °C	pH 9 37 °C	pH 7.4 60 °C
3:6	instantaneous	105	ND	ND	16	ND	ND
3:15	ND	55	45	8.6	14	13.5	10

[a]Half-life of HMVK when incubated at a concentration of 3 mM at pH 7.4, 37 °C in the absence of nucleophilic amino acids was determined to be 710 min. ND, not determined. Half-lives were estimated assuming pseudo-first order kinetics. Data is representative of typical experimental values.

Table 2

^{1}H NMR Data (chemical shifts in ppm) for major HMVK adducts with NAC and L-valinamide

	HMVK-NAC Adduct	HMVK-Valinamide Adduct
C-1[a]	2.05 (s, 3H)[b]	1.00 (d, 3H)
C-2	-	1.06 (d, 3H)
C-3	4.55 (dd, 1H)	2.22 (m, 1H)
C-4	-	3.80 (d, 1H)
C-5	2.92 (dd, 1H), 3.08 (dd, 1H)	-
C-6−7	2.80 (m, 4H)	2.96 (t, 2H), 3.32 (m, 2H)
C-9	4.33 (s, 2H)	4.34 (s, 2H)

[a] For structural assignments, see the scheme shown in Figure 5

[b] Multiplicities and integration, respectively, are listed in parenthesis

Table 3

^{1}H NMR Data (chemical shifts in ppm) for HMVK adducts with NAL

	HMVK-NAL Adduct 1	HMVK-NAL Adduct 2	HMVK-NAL Adduct 3
C-1[a]	2.00 (s, 3H)[b]	2.00 (s, 3H)	1.92 (s, 3H), (22[c])
C-3	4.28 (m, 1H)	4.26 (s, br, 1H)	4.05 (m, 1H), (55)
C-5−7	1.44, 1.69 (m, 6H)	1.40, 1.72, 1.85 (m, 6H)	1.30, 1.65 (m, 6H), (22, 24, 31)
C-8	2.93 (t, 2H)	2.45 (t, 2H)	2.53 (s, br, 2H), (23)
C-9	3.04 (t, 2H)	3.57 (s, 2H)	3.65 (m, 2H), (47)
C-10	3.29 (t, 2H)	3.15 (m, 4H)[d]	2.96 (m, 2H), (57)
C-12	4.35 (s, 2H)	2.60 (s, 1H)	-
C-14	-	3.40 (d, 1H), 3.61 (d, 1H)	5.17 (s, 1H), (91)
C-15	-	3.15 (m, 4 H)	3.15 (m, 2H), (48)
C-16	-	3.70 (d, 1H), 3.91 (d, 1H)	4.37 (d, 1H), 4.55 (d, 1H), (62)

[a] For structural assignments, see the scheme shown in Figure 7

[b] Multiplicities and integration, respectively, are listed in parenthesis

[c] Chemical shift of C based on HSQC NMR for HMVK-NAL Adduct 3

[d] Protons of C-10 and C-15 are part of the same multiplet for adduct 2